Scripta Materialia 159 (2019) 128–132

Contents lists available at ScienceDirect

Scripta Materialia

journal homepage: www.elsevier.com/locate/scriptamat

Faceting recrystallization nucleation in nanolaminated structure

H.W. Zhang [a,b,*], H. Xie [b], G.L. Wu [c], K. Lu [b]

[a] National Engineering Research Center for Equipment and Technology of Cold Strip Rolling, College of Mechanical Engineering, Yanshan University, Qinhuangdao 066004, China
[b] Shenyang National Laboratory for Materials Science, Institute of Metal Research, Chinese Academy of Sciences, Shenyang 110016, China
[c] International Joint Laboratory for Light Alloys (MOE), College of Materials Science and Engineering, Chongqing University, Chongqing 400044, China

ARTICLE INFO

Article history:
Received 28 June 2018
Received in revised form 9 September 2018
Accepted 14 September 2018
Available online xxxx

Keywords:
Nanolaminated structure
Brass orientation
Recrystallization
Faceting nucleation
Orientation gradient

ABSTRACT

A nanolaminated structure that is predominated by nanoscale lamellar boundaries with misorientations <15° was fabricated in a Brass orientated nickel single crystal. Upon annealing, {111}-aligned facets of small misorientations were formed locally in the lamellar boundaries. The subsequent migration of these facets in regions with orientation gradients accumulates large misorientations and maintains good alignment with {111}-crystallographic planes, leading to formation of rhombic nuclei bordered by high angle facet boundaries. A faceting recrystallization nucleation was proposed and the underlying mechanisms were analysed.

Recrystallization nucleation has been of great technological importance and scientific interests owing to the close relevance to the final microstructure, texture and properties of thermo-mechanically processed engineering materials [1]. A nucleus was defined as a crystallite of low internal energy growing into the adjacent deformed or recovered materials from which it is separated by high angle boundaries [1–3]. The generation and the subsequent growth of the defect-free crystallites are governed by deformation microstructures and its recovery behaviours. For the deformation microstructure that is characterized by mainly low angle cell boundaries or subgrain boundaries, recovery process for instance annihilation of dislocations, migration or coalescence of these low angle subgrain boundaries or cell boundaries is responsible for the nucleation process [4,5]. For the highly deformed lamellar structure composed of high density of high angle boundaries (>60–70 [6,7], the generation and the growth of defect-free crystals has been ascribed to the activities relevant to high angle lamellar boundaries [8] or mobile triple junctions composed of three high angle lamellar boundaries [9].

Recently, a nanolaminated structure has drawn research attention, owing to the ultrahigh hardness and thermal stability that are unreachable for other deformation microstructures [10,11]. This microstructure is characterized by nano-scale lamellar boundaries with mainly low misorientations <15°. Nanolaminated structure with an average boundary spacing of 20 nm fabricated in a pure Ni by surface mechanical grinding treatment shows a hardness of 6.4 GPa and an onset temperature for structural coarsening of 506 °C, both are substantially higher than those of ultrafine grained counterparts induced by plastic deformation with ultrahigh strains [10]. It is demonstrated that the recovery of such nanoscale low angle lamellar boundaries is characterized by the formation and growth of nano-to-submicron scale facets that are aligned with the {111}-closely compacted crystallographic planes [12,13]. Such a recovery process is expected to influence the recrystallization nucleation process, which will in the present investigation be addressed, with more emphasis on the migration and the misorientation accumulation of the facet boundaries. A faceting nucleation mechanism that differs from the traditional nucleation mechanisms was observed and the underlying causes were discussed.

A single crystal nickel (99. 945 wt% purity) with a Brass orientation, $(110)[1\bar{1}\bar{2}]$, was chosen as the experimental material. The sample was firstly fabricated into cuboid with dimensions of 10.0 × 8.0 × 6.8 mm^3. Then, the sample was plastically deformed by high strain rate compression via channel die dynamic plastic deformation (DPD) to a von Mises equivalent strain (ε_{vM}) of 3.0 with a strain rate of 10^2–10^3 s^{-1}. An extra equivalent strain of ~1.0 with a strain rate of 10°–10^1 s^{-1} was followed by cold rolling (CR). The compression direction and the normal direction (ND) are parallel with [110], while the rolling direction (RD) and the transverse direction (TD) are aligned with $[1\bar{1}\bar{2}]$ and $[1\bar{1}1]$, respectively. Recrystallization nucleation was investigated via in-situ annealing in the transmission electron microscope (TEM) and ex-situ annealing of bulk samples, respectively. A TEM sample was heated up

* Corresponding author at: National Engineering Research Center for Equipment and Technology of Cold Strip Rolling, College of Mechanical Engineering, Yanshan University, Qinhuangdao 066004, China.
E-mail address: hwzhang@ysu.edu.cn (H.W. Zhang).

https://doi.org/10.1016/j.scriptamat.2018.09.021
1359-6462/

to 450 °C with a rate of 1 °C/s and held for various times, during which the structural evolution was followed and recorded. A bulk sample was annealed in vacuum at 400 °C for 1 h, followed by cooling into water. The detailed information can be found elsewhere [12].

Structural characterizations for the deformed and annealed samples were performed on the RD-ND plane in JEM 2010 and 2100 TEMs and a FEI scanning electron microscope (SEM). Convergent beam electron diffraction (CBED) in the JEM 2010 TEM and electron backscatter diffraction (EBSD) using a HKL channel 5 detector in the SEM of the Electron Microscope Center in Chongqing University were used to quantify the microstructure like crystallographic orientations, boundary misorientations and orientation gradients. CBED offers a high angular resolution of ~0.1° through analysing the Kikuchi pattern in the TEM, which was detailed elsewhere [14,15]. EBSD allows good statistics by mapping large areas with a fine step size of 20 nm.

From Fig. 1(a), a nanolaminated structure was fabricated in the Brass orientated Ni single crystal subjected to DPD + CR to a total equivalent strain of 4.0. The dominant structural feature is the long and parallel lamellae that are roughly perpendicular to ND. The lamellae are averaged 79 nm in thickness but hundreds to thousands of nanometers in length, giving rise to an aspect ratio of the order of 10^1–10^2, which is substantially larger than that of the lamellar boundaries in highly deformed pure Ni [6,7]. Majority of the lamellar boundaries are low angle boundaries with misorientations significantly smaller than 15°, as reflected by the thin red lines on the EBSD map in Fig. 1(b) and the point-to-point misorientations distribution along three lines (black dashed lines) in Fig. 1(c). On the contrary, high angle boundaries (thick black lines in Fig. 1(b)) account for 7%, substantially lower than that (>60–70%) in heavily deformed polycrystalline metals [6,7,16]. These small amount of high angle boundaries lead to the abrupt rises in the misorientation profiles in the point-to-origin misorientation distributions (red solid lines in Fig. 1(c)), giving large local orientation variation, for instance, 13°/μm in Line 1, 16°/μm in Line 2 and 15°/μm in Line 3. This implies that Brass orientation under the present plastic deformation is stable against crystal rotation, agreeing with previous investigation [17].

The microstructural evolution of an area during the in-situ annealing in the TEM was shown in Fig. 2, where six lamellar boundaries are seen having low misorientations between them. After annealing at 450 °C for 3 min (Fig. 2(b)), two small cusps were formed locally on a straight lamellar boundary with a misorientation angle of 9.8°, whereas the adjacent lamellar boundaries with smaller misorientation angles (4.2°, 3.7° and 5.6°) remain unchanged. Compared with the initial position of the lamellar boundary (dashed lines in Fig. 2(b)), the two cusps have evolved toward its neighbouring lamella and encountered the boundary misoriented by 5.6°, producing two pairs of Y-typed triple junctions, i.e. J_1-J_2 and J_3-J_4. Upon further annealing, the two triple junctions of each pair migrated oppositely, and the curved boundaries were flattened and the cusps grow. After annealing for 43 min (Fig. 2(c)), J_2 and J_3 were merged together, forming a flat boundary that deviates a small angle from {111}-crystallographic planes (indicated by white lines in Fig. 2(e)). Prolonging annealing to 134 min (Fig. 2(d)), cusp evolves toward another lamella and encountered the boundary with a misorientation angle of 3.7°, two new Y-typed triple junctions (indicates by empty triangle) were formed. These triple junctions together with the old ones experienced migration during the subsequent annealing to 160 min, leading to a crystallite with flat facet boundary that are aligned with {111} planes (Fig. 2(e)).

Accompanied with the growth of the facet crystal via migration of facet boundaries, misorientations were accumulated and finally high angle facet boundary was formed. As evidenced by TEM observation in

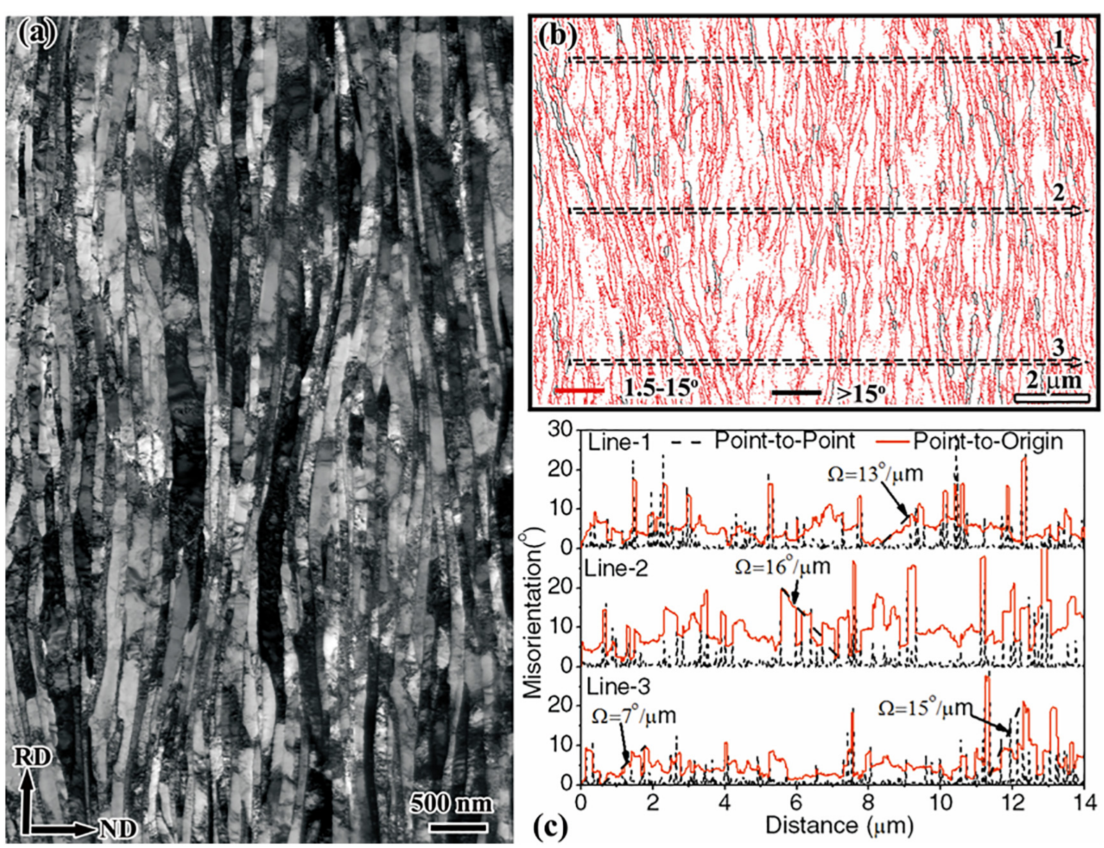

Fig. 1. Deformation microstructure of Brass-orientated single crystal Ni: (a) TEM image, (b) a boundary map reconstructed from EBSD data, and (c) the variation of the misorientation (point-to-point and point to origin) as a function of distance along the three lines parallel with ND in (b). (For interpretation of the references to color in this figure, the reader is referred to the web version of this article.)